



Zincate-Free, Electroless Nickel Deposition on Aluminum Bond Pads

James F. Rohan,^{*z} Patricia A. Murphy,^a and John Barrett^b

NMRC, National University of Ireland, Cork, Lee Maltings, Prospect Row, Cork, Ireland

A zincate-free electroless nickel deposition on aluminum bond pads is investigated. A three-step, etch, rinse, and electroless plating, is demonstrated for deposition on aluminum bond pads patterned with polyimide. The chemicals used are compatible with this dielectric material. The deposition has been achieved with good selectivity, uniformity, and deposition rate at $40 \times 40 \mu\text{m}$ aluminum bond pads. The adhesion and contact resistance were also determined and improved through anneals in the range $200\text{--}400^\circ\text{C}$ for 1 h. The optimized condition for adhesion and contact resistance was an anneal at 400°C . The combination of a nickel hypophosphite reducing agent and the additives used leads to an active plating bath in the early stages of deposition, by comparison with commercial solutions, and hence, good coverage of the aluminum bond pad using the simplified process.
© 2004 The Electrochemical Society. [DOI: 10.1149/1.1836131] All rights reserved.

Manuscript submitted March 15, 2004; revised manuscript received June 16, 2004. Available electronically December 2, 2004.

Electroless nickel deposition on aluminum usually requires a series of pretreatment steps to ensure good quality deposits. The pretreatments are necessary to remove the native surface oxide film on the aluminum and to prevent reoxidation of the etched aluminum. The most common pretreatment employed in industry¹ and more recently in chip-bump processing²⁻⁶ is the zincate treatment which involves immersion of the aluminum substrate in a concentrated sodium hydroxide-based solution containing zinc ions which removes the oxide and deposits a protective zinc layer. It is usually necessary to repeat the process to obtain the best quality coverage. Upon immersion in the electroless nickel plating solution, the zinc dissolves and is replaced by nickel ions, which initiates the autocatalytic deposition of nickel directly at the aluminum surface. In microelectronics applications this process has some potential drawbacks, including process complexity and the exposure of the substrate to undesirable metal ion contaminants such as zinc. For these reasons alternative activations of the aluminum substrate for electroless nickel deposition have been investigated, such as HF etching,⁷ deaerated rinsing solutions, and displacement nickel deposition or activation by dimethyl amine borane (DMAB) solution,⁸ and laser irradiation of the aluminum to remove anodically formed oxide.⁹ An additional process step, the deposition of a thin Ni-B base layer from alkaline solutions, has also been required in some cases^{4,8} before deposition from the more common hypophosphite could take place. This paper describes a simple etch, rinse, and plating process for the selective deposition of electroless Ni-P bumps on aluminum bond pads for use in flip-chip assembly.

Experimental

All experiments were performed in glass beakers with magnetic stirring at 100 rpm. The plating solution was heated on a hot plate with a Teflon-coated temperature probe to maintain a constant temperature. The pH was adjusted using ammonium hydroxide to the required value at room temperature and then heated to the operating temperature. Teflon substrate holders were used. The substrates were patterned aluminum ($1.5 \mu\text{m}$ thick) bond pads ($40 \times 40 \mu\text{m}$) deposited using an Endura AMAT 5500 physical deposition tool. The patterning material was $3 \mu\text{m}$ thick polyimide (PI). The deposit selectivity and morphology were analyzed using a Hitachi S-400 field effect scanning electron microscope (SEM) with a PGT IMIX energy-dispersive X-ray (EDX) system with intensity correction for elemental analysis of deposit composition and uniformity. Deposit height and uniformity was determined using a Tencor Alpha-Step 200 surface profilometer and correlated with data recorded on the SEM. Samples were annealed under a nitrogen ambient in a solder

reflow over (SRO 702) by ATV Technology, Inc. The adhesion of $40 \mu\text{m}$ high nickel bumps was measured using a Dage BT 24 shear tester from Dage Precision Industries, Inc. (CA). In these tests nickel bumps were sheared from the aluminum substrate using a $100 \mu\text{m}$ tool head which has a lead edge perpendicular to the substrate and travels parallel to the substrate at a rate of $500 \mu\text{m/s}$ at a height of $5\text{--}10 \mu\text{m}$. The force to shear the bump recorded is the average of 15 tests for each substrate.

An alkaline etch composed of 50 mL each of H_2O_2 and NH_4OH of the concentrates (30% semiconductor grade, supplied by Ashland Chemicals, OH) in 1 L of deionized water was used to clean the aluminum surface and remove the oxide layer. An optimized etch time of 30 s removed $0.3 \mu\text{m}$ of aluminum; the native aluminum oxide was removed and the surface was slightly roughened. The use of an alkaline etch step in the plating process was critical to the activation of the aluminum bond pads to electroless nickel plating. After etching, the wafer was immediately rinsed in propan-2-ol. This solvent rinse was used, rather than an aqueous rinse, to help prevent the reoxidation of the fresh aluminum surface. The sample was transferred directly from the solvent to the plating solution. The plating bath operates at a temperature of $87\text{--}90^\circ\text{C}$ and the boiling point of propan-2-ol is 84.2°C ; thus, any propan-2-ol remaining on the aluminum pads after the solvent rinse evaporates on immersion of the samples into the plating bath. An electroless nickel bath formulated from its constituents (Table I), and three commercial baths were examined. Details for the commercial solutions have been described earlier.¹⁰ All baths were based on a hypophosphite reducing agent and operated at a pH of $4.0\text{--}5.0$. The bath in Table I was also designed to be sodium ion-free, utilizing nickel hypophosphite as the reducing agent. This electroless nickel bath afforded selective uniform plating on the aluminum bond pads. The commercial electroless nickel baths were not sufficiently active to initiate nickel plating on the aluminum surface using the simplified alkaline etch and solvent rinse process.

Results and Discussion

Plating process.—Nickel bumps were selectively deposited using a simple process that did not require the use of an additional metal deposition step such as occurs in the standard zincate process.

Table I. The composition of the electroless nickel bath.

Chemical	Molarity
Nickel sulfate	0.05
Ammonium sulfate	0.25
Nickel hypophosphite	0.13
Lactic acid	0.22
Calcium succinate	0.01
pH	$4.0\text{--}5.0$
Temperature	$85\text{--}95^\circ\text{C}$

* Electrochemical Society Active Member.

^a Present address: Intel Ireland Ltd., Leixlip, County Kildare, Ireland.

^b Present address: Cork Institute of Technology, Bishopstown, Cork, Ireland.

^z E-mail: james.rohan@nmrc.ie

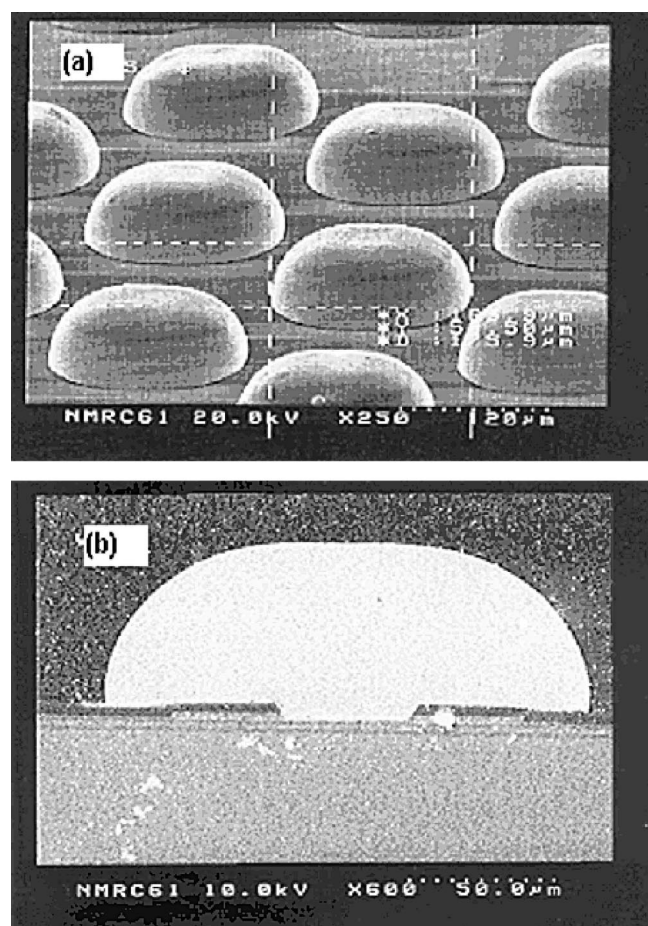


Figure 1. Selective electroless nickel bumps deposited in 3 h plating on aluminum $40 \times 40 \mu\text{m}$ bond pads: (a) SEM image of nickel bump array and (b) cross section of a nickel deposit.

The plating process utilized consisted of an etch step and a solvent rinse prior to plating. This metal deposition method has a number of advantages over other aluminum activation processes such as zincation or palladium activations. First, the sample is not exposed to additional species such as zinc, sodium, or palladium, and second, the process is selective and the rear of the wafer is not plated.

Initial plating experiments using the acidic nickel bath operating at a pH of 4.2 and operating temperature of 85°C afforded nickel plating at a typical rate of $8 \mu\text{m/h}$. Increasing the operating temperature to 90°C and solution pH to 4.6 increased the deposition rate to $20 \mu\text{m/h}$. Figure 1 illustrates a selectively plated array of $58 \mu\text{m}$ high nickel bumps on a wafer that was plated in the acidic nickel bath for 3 h. The plating uniformity of the electrolessly deposited bumps is indicated in Table II, which lists the mean and standard deviation for 30 sites on the substrate. The data indicates that the deposit uniformity is maintained over extended deposition times.

Adhesion.—In electroless plating, deposition commences autocatalytically only on the patterned aluminum of the bond pad. Additional photolithographic patterning is not required. This is a significant advantage of the electroless process. However, the deposit

Table II. Nickel bump height uniformity.

Sample	Number of measurement sites	Mean bump height (μm)	Standard deviation (μm)
1	30	52.52	1.61
2	30	51.90	2.40

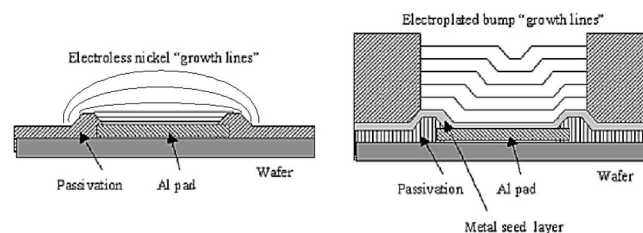


Figure 2. Growth lines for electroless and electrolytic deposits on aluminum bond pads.

grows both vertically and laterally at the same rate as shown in the cross-sectional SEM image of Fig. 2. The lateral growth causes the bump to spread onto the passivation surrounding the aluminum bond pad. The adhesion of this lateral plating to the passivation, in this case PI, may be low. In electrolytic metallization of bond pads, a metal seed layer is deposited which covers both the aluminum bond pad and the passivation. Photolithography is used to constrain bump growth to the required areas over the bond pads and the bump material is deposited only over metal which provides adequate adhesion. The nickel-to-aluminum adhesion required from electrolessly plated deposits therefore must be greater than the comparable bump plated by electrolytic means. To improve the bump-wafer adhesion with electroless plating, either the nickel to passivation or the nickel to aluminum adhesion, or both, must be increased.

Chemical and physical modification of the PI prior to plating was studied as a method to increase the Ni-PI adhesion. The factors examined in order to increase the Ni-Al adhesion included improving the plating process and annealing the samples after plating. Initial bump shear strength tests indicated that the bump-to-wafer adhesion strength was 35 g per pad for the $40 \times 40 \mu\text{m}$ metal connection, when the nickel was deposited at pH 4.2 and a plating bath temperature of 85°C . The results of the bath operating conditions and substrate treatments which lead to a large increase in nickel-to-wafer adhesion are given in Table III.

The physical treatments to roughen the PI surface included an oxygen plasma ash and abrasion of the surface using silicon carbide paper. The SEM image in Fig. 3 illustrates the surface of the PI following abrasion using silicon carbide paper. All treatments that roughen the PI surface lead to an increase in adhesion shear strength. Oxygen plasma etching of the PI prior to plating afforded the largest shear strength increase; a value of 130 g/pad was measured which compares very favorably with shear strength values quoted for electroless nickel bumps.⁵ Chemical treatments included alkaline and acid solutions and an *n*-methyl-pyrrolidinone (NMP) dip. NMP is used to strip PI at elevated temperatures and softens the material at lower temperatures. Chemical treatment of the samples prior to plating did not, however, lead to an increase in the bump-wafer adhesion.

To further improve the overall adhesion, the effect of annealing on the plated die was also examined. Samples were annealed at a range of temperatures between 200 and 400°C . Annealing was found

Table III. Adhesion data for nickel deposits on substrates subjected to listed treatment.

Treatment	Deposit height (μm)	Shear strength (g per pad)	Standard deviation (g per pad)
Untreated sample	40	66.0	11.1
Oxygen plasma etch	45	130.1	8.3
Abrasion 4000 grit SiC	30	84.8	4.2
Abrasion 2500 grit SiC	30	89.6	5.1
Abrasion 1200 grit SiC	30	95.7	4.0
Anneal 200°C	40	61.8	7.2
Anneal 300°C	40	95.2	21.1
Anneal 400°C	40	173.2	30.7

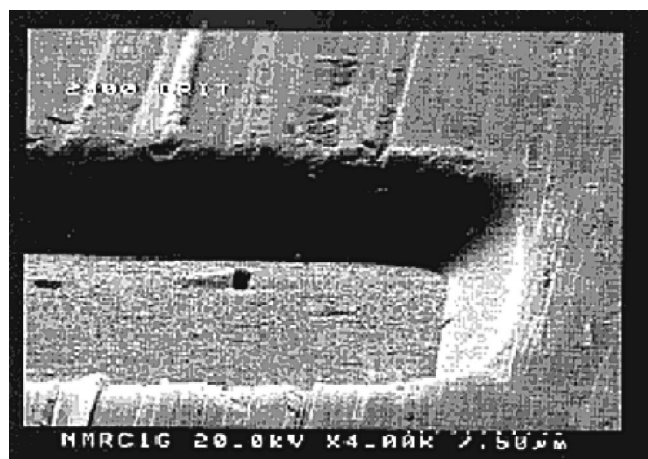


Figure 3. SEM image is of an aluminum bond pad and polyimide after abrasion using 4000 grit silicon carbide paper.

to increase the nickel-to-aluminum adhesion, with higher anneal temperatures affording the greatest increase in adhesion. Shear strengths of 170 g/pad were measured when samples were annealed at 400°C in an oxygen-free environment for 1 h, again indicating good adhesion for the small pad size.

SEM analysis was also used to examine the aluminum bond pads of plated samples where the nickel bumps had been removed during shear testing. Where samples had been annealed the surface of the aluminum was rougher than samples that had not been heat-treated. No nickel was detected by EDX at the bond pad following shear test. This suggests that annealing the samples causes a localized interaction between the nickel and the aluminum bond pads. This interaction probably accounts for the increase in adhesion upon annealing. Figure 4a and b shows SEM images of aluminum bond pads for plated samples where the nickel bumps have been removed by shear testing. The sample in Fig. 4a was not annealed while the sample in Fig. 4b has been annealed at 400°C prior to shear testing.

Auger analysis.—Auger depth profiling of a series of samples as plated and after anneals at 200, 300, and 400°C did not show significant interdiffusion at the Ni/Al interface. The profiled samples were plated with a thin nickel deposit ($\sim 5 \mu\text{m}$ thick). Auger spectra were acquired affording detailed information on the composition of the nickel/aluminum interface. Comparing the spectra of the sample as-plated and annealed at 400°C showed no detectable variation in peak shape or shift at the interface areas. This suggests that the oxidation states of nickel and aluminum do not change around the interface region, and thus intermetallic compounds are not being formed. Figure 5a and b illustrates the depth profiles of atomic composition of an as-plated sample and a sample annealed at 400°C. In the spectra the Al is observed at the right side of the spectra, the nickel and phosphorous are seen on the left side, and the oxygen signal is at the bottom of the spectra. These results were supported by EDX line scans which did not indicate a significant concentration change at the interface following an anneal at 200–400°C.

Resistance measurements.—The contact resistance between the deposited electroless nickel and the underlying aluminum of the wafer was investigated using two-point probe resistance measurements. These measurements were carried out on bumped wafers that had not been annealed and on samples that were annealed at temperatures of 200, 300, and 400°C. Test structures (Fig. 6) measured on the substrate involved multiple nickel-aluminum daisy chained contacts. Using this structure, the resistance of many Ni/Al interfaces and Al links can be measured at one time with a two-probe system. Measurements at this test structure provide a better representation of the resistance of the system, as the interfaces are not influenced by the pressure applied to the deposit during probing.

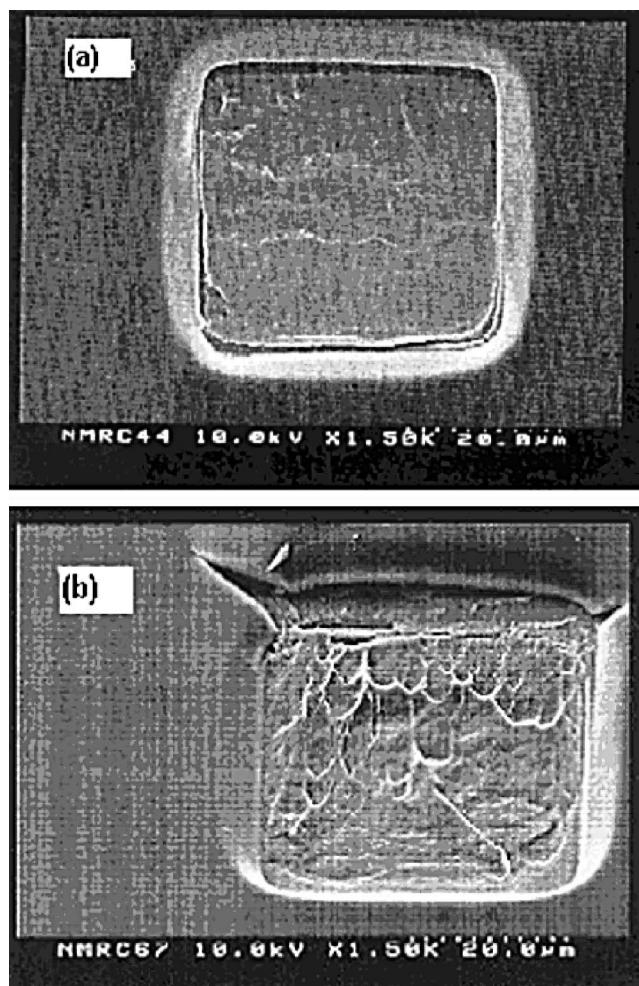


Figure 4. SEM images of aluminum bond pads of plated samples where the nickel bumps had been removed: (a) no heat-treatment and (b) annealed at 400°C prior to shear testing. No nickel was detected at the remaining aluminum of the bond pad.

The resistance values measured on a series of samples are illustrated in Fig. 7. The resistance measured vs. the number of Ni/Al interfaces is plotted for a series of samples that were measured as-plated and annealed at 200, 300, and 400°C. All the resistance values measured indicate a low Ni/Al contact resistance per bond pad. Annealing the samples affords a reduction in resistance values at the Ni/Al interface. In Fig. 7 a dramatic decrease in resistance was observed when samples were annealed at 400°C. Based on previous analysis,¹¹ the crystallization of the electroless nickel deposit may be the factor contributing most to this result.

Based on the plating observations and deposit analysis, it is proposed that the peroxide/ammonia etchant removes the oxide at the surface of the aluminum, as indicated by the 0.3 μm decrease in aluminum pad height following this treatment. The etched aluminum surface is protected from reoxidation by immersion in the nonaqueous rinse solvent, which is similar to the protection afforded by zinc in the standard zincation process. This solvent also protects the aluminum surface during transfer to the nickel plating bath and during the initial seconds of immersion in that bath. The zincate process affords a more durable protection and is better suited to the full range of substrate dimensions. The solvent protection described in this work protects the relatively small pad area adequately during the time scale of removal from the solvent rinse and immersion in the plating bath. Once in the plating solution the exposed aluminum surface is most likely involved in a displacement reaction with the nickel ions, again in a mechanism similar to that which occurs fol-

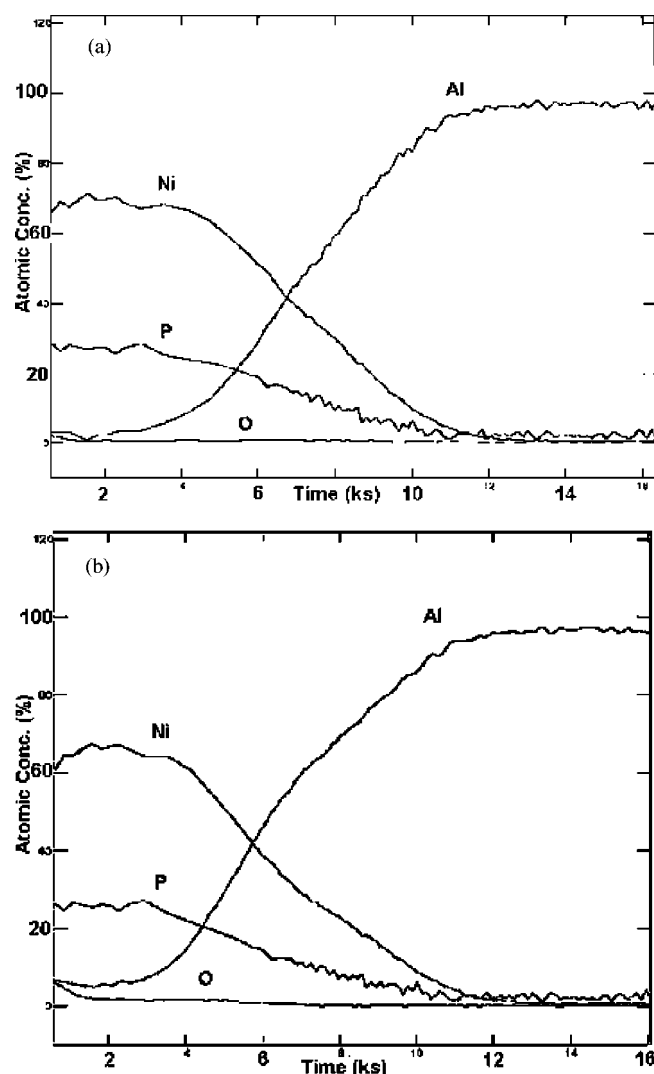


Figure 5. (a, top) Auger depth profiles of atomic composition of the Ni/Al interfaces of samples as-plated and (b, bottom) after annealing at 400°C.

lowing zinc dissolution in the zincate process, given the potential difference between the aluminum dissolution and nickel-ion reduction reactions. The plating bath used is more active for nickel deposition at the operating pH of 4.6 and temperature of 90°C (20 $\mu\text{m/h}$ achieved) than at a pH of 4.2 and temperature of 85°C (8 $\mu\text{m/h}$ achieved), and more active than commercial solutions which did not yield deposits using this technique. This may be due to the lower additive content for the bath described in this work, which can yield deposits at 20 $\mu\text{m/h}$ from the zincate-free process. Therefore, it would appear that the critical displacement and subsequent autocata-

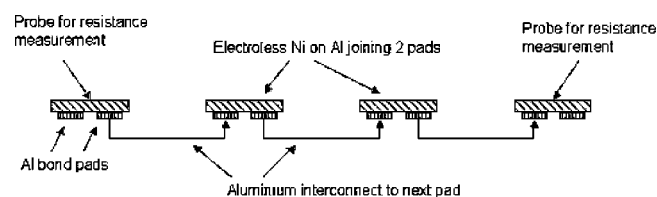


Figure 6. Schematic of the daisy chain layout with aluminum pads connected along the chain through electroless nickel deposit. Probing for resistance is performed only at the start and end of chain, permitting the determination of the resistance of a series of nickel/aluminum interfaces.

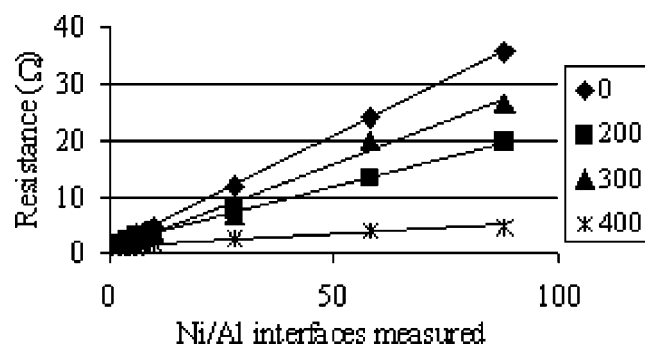


Figure 7. Resistance measurements vs. Ni/Al interfaces. Samples as-plated and after annealing at 200, 300, and 400°C.

lytic deposition that occurs in the early stages (0.3 $\mu\text{m/min}$ expected by extrapolating from the long term deposition experiments) does so in a uniform manner across the bond pads at a high rate before the aluminum reoxidizes. In addition to the increased deposition rate under the optimized plating conditions, shear test analysis indicated that the nickel has better adhesion to the aluminum when the nickel is deposited at a higher rate. This most likely results from direct nickel-to-aluminum contact, which occurs at a substantially oxide-free surface.

Conclusions

A zincate-free route for electroless nickel direct deposition on aluminum bond pads has been demonstrated. This technique is significantly simpler, requiring only three steps, than the standard zincate process and does not require the use of hazardous chemicals, such as HF, employed in some cases as an alternative to the zincate treatment. It also affords selective deposition which may not be achieved using Pd or other such activating solutions to assist the initial deposition on the aluminum. The deposition has been achieved with good selectivity, uniformity, and at a relatively high deposition rate of 20 $\mu\text{m/h}$ at $40 \times 40 \mu\text{m}$ aluminum bond pads. For flip-chip applications where the electroless nickel acts as an under-bump metallurgy, adhesion and contact resistance are significant factors. These have been determined and optimized through anneals in the range 200–400°C for 1 h. Similar selective deposition was not achievable with commercial plating solutions using this three-step process. It is suggested that the combination of the active plating bath with few additives, comprising a nickel hypophosphite reducing agent, leads to a more active plating bath in the early stages of deposition and hence, good coverage of the aluminum bond pad using the simplified process described.

Acknowledgments

This work was funded in part by Intel and Enterprise, Ireland, under grant no. HE/98/262.

The National University of Ireland, Cork, assisted in meeting the publication costs of this article.

References

1. J. B. Hajdu, *Electroless Plating: Fundamentals and Applications*, Chap. 7, G. O. Mallory and J. B. Hajdu, Editors, American Electroplaters and Surface Finishers Society Publishers, Orlando, FL (1990).
2. K. Wong, K. Chi, and A. Rangappan, *Plat. Surf. Finish.*, **7**, 70 (1988).
3. J. Liu, *Hybrid Circ.*, **29**, 25 (1992).
4. A. M. T. van der Putten and J. W. G. de Bakker, *J. Electrochem. Soc.*, **140**, 2229 (1993).
5. Y.-D. Jeon and K.-W. Paik, *IEEE Trans. Compon. Packag. Technol.*, **25**, 169 (2002).
6. A. J. G. Strandjord, S. Popelar, and C. Jauernig, *Microelectron. Reliab.*, **42**, 265 (2002).
7. C. H. Ting, M. Paunovic, P. L. Pai, and G. Chiu, *J. Electrochem. Soc.*, **136**, 462 (1989).
8. H. Watanabe and H. Honma, *J. Electrochem. Soc.*, **144**, 471 (1997).
9. S. Z. Chu, M. Sakairi, H. Takahashi, and Z. X. Qiu, *J. Electrochem. Soc.*, **146**, 537 (1999).
10. J. F. Rohan, G. O'Riordan, and J. Boardman, *Appl. Surf. Sci.*, **185**, 289 (2002).
11. J. F. Rohan and G. O'Riordan, *Microelectron. Eng.*, **65**, 77 (2003).